Journal of Nuclear Medicine, published on February 17, 2022 as doi:10.2967/jnumed.121.263132

^{68}Ga-DOTA-NT-20.3 Neurotensin receptor 1 positron emission tomography imaging as a surrogate for neuroendocrine differentiation of prostate cancer

Wenyu Wu[1], Fei Yu[1], Pengjun Zhang[1], Ting Bu[1], Jingjing Fu[1], Shuyue Ai[1], Qinqin You[1], Liang Shi[1], Guoqiang Shao[1], Feng Wang*[1], Marina Hodolic*[2,3], Hongqian Guo[4]

[1] Department of Nuclear Medicine, Nanjing First Hospital, Nanjing Medical University, Nanjing, China; [2] Nuclear Medicine Research Department, IASON, Graz, Austria; [3] Department of Nuclear Medicine, Faculty of Medicine and Dentistry, Palacký University Olomouc, Olomouc, Czech Republic; and [4]Department of Urology, Drum Tower Hospital, Medical School of Nanjing University, Institute of Urology, Nanjing University, Nanjing, China

* Correspondence to Feng Wang, PhD. Department of Nuclear Medicine, Nanjing First Hospital, Nanjing Medical University, 68th Changle Road, Nanjing, China, 210006.
E-mail: fengwangcn@hotmail.com, fengwangcn@njmu.edu.cn
* Marina Hodolic, M.D. Department of Nuclear Medicine, Faculty of Medicine and Dentistry, Palacký University Olomouc, Olomouc, Czech Republic.
E-mail: marina.hodolic@gmail.com

Running Title: NTR1 imaging for neuroendocrine PCa

ABSTRACT

PSMA-negative neuroendocrine prostate cancer (NEPC) is likely to be a lethal subtype of prostate cancer (PCa) with limited clinical diagnostic and therapeutic options. High expression of neurotensin receptor subtype 1 (NTR1) associated with neuroendocrine differentiation of PCa, which makes NTR1 a potential target for NEPC. In this study, NTR1-targeted tracer ^{68}Ga-DOTA-NT-20.3 was synthesized and evaluated by determining its affinity to androgen-dependent (LNCap) and androgen-independent (PC3) xenografts. **Methods:** ^{68}Ga-DOTA-NT-20.3 was labeled with an automated iQS-theranostics synthesizer module and its stability, labeling yield, and radiochemical purity were analyzed by radio-HPLC. Receptor binding affinity was evaluated in NTR1-positive PC3 cells by competitive binding assay. The biodistribution of ^{68}Ga-DOTA-NT-20.3 *in vivo* was evaluated in PC3 and LNCap xenografts by micro-PET imaging. NTR1 expression was identified by immunohistochemistry and immunofluorescence. **Results**: ^{68}Ga-DOTA-NT-20.3 was synthesized successfully with a yield rate of 88.07 ± 1.26 %, radiochemical purity ≥ 99% and favorable stability. The NTR1 affinity (IC_{50}) for ^{68}Ga-DOTA-NT-20.3 was 7.59 ± 0.41 nM. Micro-PET/CT in PC3 xenografts showed high contrast images with intense tumor uptake, which revealed specific NTR1 expression. The tumor showed significant radioactivity (4.95 ± 0.67 percentage of injected dose per gram of tissue [%ID/g]) at 1h, which fell to 1.95 ± 0.17 %ID/g ($P < 0.01$, $t = 8.72$) after specific blockage by neurotensin. LNCap xenografts had no significant accumulation (0.81 ± 0.06 %ID/g) of ^{68}Ga-DOTA-NT-20.3 at 1 h. In contrast, ^{68}Ga-PSMA-11 was mainly concentrated in LNCap xenografts (8.60 ± 2.11 %ID/g), with no significant uptake in PC3 tumors (0.53 ± 0.05 %ID/g), consistent with the *in vitro* immunohistochemistry findings. Biodistribution showed rapid clearance from the blood and main organs (brain, heart, lung, liver, muscle, bone) with significantly high tumor/liver (4.41 ± 0.73) and tumor/muscle ratios (12.34 ± 1.32) at 60 min post-injection. **Conclusion:** ^{68}Ga-DOTA-NT-20.3 can be efficiently prepared with a high yield and radiochemical purity. Its favorable biodistribution and prominent NTR1 affinity make ^{68}Ga-DOTA-NT-20.3 a potential radiopharmaceutical for the detection of PSMA-negative PCa and identification of neuroendocrine differentiation.

Key words: ^{68}Ga-DOTA-NT-20.3; neurotensin receptor subtype 1; prostate cancer; neuroendocrine differentiation; PET

INTRODUCTION

The incidence of prostate cancer (PCa) has increased in line with the aging population and progress in diagnostic modalities (*1*). Patients usually have advanced or metastatic lesions at diagnosis, leading to high mortality. PSA has been well documented for the diagnosis of PCa and evaluation of tumor response (*2*). However, PSA increase is largely dependent on the tumor origin, and PSA can be increased in benign prostatic hyperplasia, likely not to increase in poorly differentiated PCa (*3,4*). PSMA PET has been widely used in clinical gradually, which had merits in the detection of biomedical recurrence, allowing the detection of micro-metastasis at low PSA values (*5*). PSMA is commonly overexpressed in metastatic castration-resistant prostate cancer (CRPC) and serves as ideal target for the treatment of PCa (*6*). However, poorly differentiated PCa originating from luminal and basal cells frequently acquires a neuroendocrine phenotype (neuroendocrine prostate cancer, NEPC), which lacks PSMA expression, following long-term ADT (*7*). Although the incidence of de novo NEPC is rare (< 2 %), treatment-driving neuroendocrine differentiation is existent in up to 20% of patients with CRPC (*8*). As an aggressive subtype of CRPC, the median survival time of patients with NEPC is < 1 year due to difficult identification and fewer treatment options owing to androgen deficiency (*9*). The lethal nature of NEPC is driven by a lack of therapeutic regimens capable of generating durable responses in the setting of extreme tumor heterogeneity at the genetic and cell biological levels. Specific molecular targets and efficient therapeutic interventions are therefore necessary explored for the clinical management of NEPC.

The neurotensin/neurotensin receptor (NT/NTR) axis has been identified as an alternative growth pathway in androgen-independent PCa and as a factor in the development of NEPC (*10*). NT is a tridecapeptide released from endocrine cells in the small bowel, which stimulates pancreatic and biliary secretion, fatty acid absorption, intestinal motility, and growth of digestive organs (*11*). Additionally, NT secreted from carcinoma cells acts as an autocrine growth factor in response to tumor cell proliferation and migration (*12*). NT functions are primarily mediated via two G-protein coupled receptors: NTR1 (high-affinity receptor) and NTR2 (low-affinity receptor), while NTR3 serves as a single transmembrane domain localized in the trans-Golgi network (*13*). NTR1 is overexpressed in neuroendocrine differentiation of PCa, and may promote neoplastic growth and metastasis after binding with NT produced by neuroendocrine cells in NEPC

(*14,15*). The latest study showed that NTR1 was expressed in 91.8% PCa tissues, and all PSMA-negative tissues showed positive NTR1 expression, suggesting the potential complementary role of NTR1-targeted imaging or therapy (*16*). LNCap (androgen-dependent PCa cell) showed negative NTR1 expression while PC-3 had positive expression (androgen-independent PCa cell). Although native NT is sensitive to peptidases, various NT analogs with higher stability have been radiolabeled and used as valuable imaging and internal radioligand therapeutic tools for NTR1-positive tumors (*17-20*). Among them, ^{68}Ga-DOTA-NT-20.3 is confirmed a promising PET imaging probe for NTR1-positive tumors such as pancreatic adenocarcinoma and colon cancer (*21, 22*). However, ^{68}Ga-DOTA-NT-20.3 PET for the quantitation of NTR1 expression in PCa underwent neuroendocrine differentiation has not been reported. In this study, ^{68}Ga-DOTA-NT-20.3 was used to evaluate the neuroendocrine differentiation status in PCa xenografts.

MATERIALS AND METHODS

General

The vender information of chemicals, cells, reagents, and animals as well as the cell culture and tumor model are provided in the Supplemental Data. All animal studies approved by Nanjing First Hospital animal ethical committee and performed according to national regulations.

Radiolabeling DOTA-NT-20.3 / PSMA-11 with ^{68}Ga and Quality Control

An iQS-TS automated module was used for all radiolabeling steps carried out as described (*21-23*) with minor modifications. Briefly, DOTA-NT-20.3 (4.32 nmol, 20 μg) or PSMA-11 (19.72 nmol, 20 μg) dissolved in 1.0 mL sodium acetate buffer (0.25 M, pH 8.0) and ^{68}Ga (370 – 450 MBq) eluted from the Ge-68/Ga-68 generator with 4.0 mL 0.05 M HCl were introduced into the preheated reactor. The final labeling solution pH was at 3.5-4.0. After reaction at 95°C for 14 min, the labeled product was concentrated using a disposable Sep-Pak C18 cartridge (Waters, Milford, USA), eluted with 0.5 mL 70% ethanol and equilibrated with 0.9% sodium chloride injection or fresh medium before used. Quality control of radiopharmaceuticals was performed using radio-HPLC and radio-TLC (details presented in Supplemental Data).

Determination of Lipophilicity

The shake-flask method was used to determine the partition coefficient of ^{68}Ga-DOTA-

NT-20.3 in *n*-octanol and PBS (pH 7.4) mixture. The organic and aqueous phases were pre-saturated 24 h before experiment, and 500 μL of each layer was added to ^{68}Ga-DOTA-NT-20.3 (3.7 MBq) and mixed vigorously for 3 min. The layers were separated by centrifugation at 2000 rpm (416 g) for 5 min. Aliquots of 100 μL were removed from each phase and measured in a Wizard gamma counter. Calculated $logD_{7.4}$ values were expressed as mean ± standard deviation (SD) from three experiments.

Stability in Vitro

For stability assay, ^{68}Ga-DOTA-NT-20.3 was incubated in PBS (pH 7.4) or fresh human serum at 37 °C for 15, 30, 60, 120 and 240 min, respectively. Plasma protein was precipitated with isovolumic acetonitrile and removed by centrifugation (12,000 rpm, 13,400 g, 5 min) after incubation. The supernatants were analyzed by radio-HPLC after filtering through a Cathivex-GV filter (22 μm; Merck, Darmstadt, Germany).

Cell Binding Affinity and Uptake Assay

Human prostate adenocarcinoma PC3 cells were seeded into 24-well plates at a density of 1×10^5 cells per well overnight for the receptor-binding affinity and uptake study of ^{68}Ga-DOTA-NT-20.3. ^{68}Ga-DOTA-NT-20.3 and NT were diluted to 37 kBq/mL and 10^{-8}–10^2 μM with fresh medium, respectively. For receptor-binding affinity assay, ^{68}Ga-DOTA-NT-20.3 (37 kBq, 500μL) was added to each well in the presence of varying concentrations (10^{-8}–10^2 μM, 500μL) NT. After incubation for 60 min at 37°C, the medium of each well was removed and cells were washed twice with PBS. The removed medium and washing PBS were collected to represent the amount of free radioligand. The adherent cells were lysed with NaOH (0.1M, 200 μL) and harvested after washed twice by PBS. Finally, the cell-bound radioactivity (3×10^5 cells/mL) as well as the amount of free radioligand were measured in a gamma-counter. The half-maximal inhibitory concentration (IC_{50}) was calculated using GraphPad Prism software. For cell uptake study, the trial group PC3 cells were incubated with ^{68}Ga-DOTA-NT-20.3 (37 kBq, 500μL) at 37°C for 15, 30, 60, and 120 min, respectively. The blocking group cells were saturated with excess NT (1 μM, 500μL) before adding ^{68}Ga-DOTA-NT-20.3 (37 kBq, 500μL). The radioactivity of adherent cells (3×10^5 cells/mL) was then measured after extracted with NaOH (0.1 M, 200 μL) and washed twice with PBS.

Micro-PET/CT Imaging

The whole-body distribution of the tracer in tumor-bearing mice was examined with an

Inveon micro-PET/CT. ^{68}Ga-DOTA-NT-20.3, ^{68}Ga-PSMA-11 and NT were diluted to 37 MBq/mL, 37 MBq/mL and 2 mg/mL with 0.9% sodium chloride injection, respectively. PC3-xenografted mice (18-25g) were injected with ^{68}Ga-DOTA-NT-20.3 (7.4 MBq, 200μL) via the tail vein under isoflurane anesthesia, and 10-min static PET images were acquired at 0.5, 1, 1.5, 2, and 4 h after injection. For the blocking group, mice were pretreated with excess NT (20 mg/kg body weight, 200μL) via tail vein 15 min prior to ^{68}Ga-DOTA-NT-20.3 (7.4 MBq, 200μL), and static PET images were acquired at 1 h post-injection. PC3- and LNCap- xenografted mice were imaged at 1 h after receiving ^{68}Ga-DOTA-NT-20.3 (7.4 MBq, 200μL) or ^{68}Ga-PSMA-11 (7.4 MBq, 200μL). Images were reconstructed using a three-dimensional ordered-subset expectation maximization protocol with attenuation correction. Regions of interest were drawn over the tumors and main organs, and average signal levels in the regions were measured using an Inveon Research Work Station.

Ex-Vivo Biodistribution

PC3 xenograft mouse models (18-25g) were used to evaluate the distribution of tracer in blood and major organs. ^{68}Ga-DOTA-NT-20.3 was diluted to 37 MBq/mL with 0.9% sodium chloride injection for use. Mice were sacrificed 5, 15, 30, 60, and 120 min after intravenous injection of ^{68}Ga-DOTA-NT-20.3 (3.4 MBq, 100μL) (n=3 per group). Blood and major organs were harvested immediately, weighed, and counted using a gamma counter. The radioactivity of each sample was calculated as the percentage of injected dose per gram of tissue (% ID/g) and corrected for radioactive decay.

Immunohistochemical Staining

NTR1 and PSMA expression were evaluated by immunohistochemistry in LNCap- and PC3- derived prostate tumors. PCa tissues were fixed in 4% paraformaldehyde, paraffin-embedded, and sectioned. The sections were then dewaxed and hydrated with xylene and graded alcohol at room temperature before heat-induced antigen retrieval. Endoperoxidase activity was inactivated by 3% H_2O_2 and nonspecific sites were blocked with 3% BSA. The sections were incubated overnight with NTR1 antibody (cat. YT3203, 1:200 dilution, ImmunoWay, USA) at 4°C followed by HRP labeled goat anti-rabbit second antibody (cat. GB23303, 1:200 dilution, Servicebio, China), then staining with 3,3-diaminobenzidine and counterstaining with hematoxylin solution for 2 min. The samples were finally dehydrated and mounted with neutral resin and images were acquired using an optical microscope (Nikon Eclipse E100, Japan).

Histological Analysis

The tissues were fixed in 4% paraformaldehyde and embedded in paraffin for sectioning. Tumor sections were dewaxed, stained with hematoxylin and eosin (H&E) fixed with neutral resin after dehydration, and observed using an optical microscope.

Immunofluorescent Staining

Cells in 12-well culture plates were fixed with 4% paraformaldehyde and permeabilized with 0.5% Triton X-100 in PBS for 20 min at room temperature. Nonspecific antibodies were blocked with 5% BSA in PBS for 30 min at room temperature. NTR1 antibody (1:100 dilution) was added to each well and incubated at 4℃ overnight to detect NTR1. The sections were then incubated with CY3 labeled goat anti-rabbit IgG secondary antibody (cat. GB21303, 1:300 dilution, Servicebio, China) followed by antifade medium containing 4,6-diamidino-2-phenylindole, and observed under a fluorescence microscope.

Statistical Analysis

Quantitative data were described as mean ± SD, and differences between groups were analyzed by Student's *t*-test or ANOVA using GraphPad Prism 6.0 software. A *P*-value < 0.05 was considered statistically significant.

RESULTS

Radiosynthesis of ^{68}Ga-DOTA-NT-20.3 and ^{68}Ga-PSMA-11

^{68}Ga-DOTA-NT-20.3 (Fig. 1) and ^{68}Ga-PSMA-11 were labeled successfully within 14 min with yield rates of 88.07 ± 1.26 % and 86.82 ± 2.57 %, respectively. The final molar activity (radioactivity of product / amount of peptide used) of ^{68}Ga-DOTA-NT-20.3 was ≥ 54.4 GBq/μmol. Radio-HPLC showed > 99 % radiochemical purity of ^{68}Ga-DOTA-NT-20.3 and ^{68}Ga-PSMA-11, and the elution time were 13.49 and 8.19 min, respectively (Supplemental Fig. 1 and 2). Radio-TLC of ^{68}Ga-DOTA-NT-20.3 showed only one spot with a retention factor of 0.60 (Supplemental Fig. 3).

Lipophilicity and In Vitro Stability

The lipophilicity of the peptide radiotracer was represented by the partition coefficient of ^{68}Ga-DOTA-NT-20.3 determined as $\log D_{7.4}$ value of −3.68 ± 0.14 in *n*-octanol and PBS. The radiochemical purity of ^{68}Ga-DOTA-NT-20.3 was still ≥ 99% after incubation in PBS and human serum at 37°C for 4 h, indicating the tracer was sufficiently stable for further *in vitro* and *in vivo* studies (Supplemental Fig. 4).

In Vitro Cell Binding Affinity and Uptake

Competitive cell binding assays revealed that NT inhibited the binding of ^{68}Ga-DOTA-NT-20.3 to NTR1-positive PC3 cells in a concentration-dependent manner (Fig. 2A). The IC_{50} value for ^{68}Ga-DOTA-NT-20.3 was 7.59 ± 0.41 nM. Cell blocking studies were conducted to evaluate the specificity of ^{68}Ga-DOTA-NT-20.3 *in vitro* (Fig. 2B). Uptake rate of ^{68}Ga-DOTA-NT-20.3 by PC3 cells reached a plateau (4.21 ± 0.33 percentage of administered dose [%AD]) at 1 h of incubation and decreased significantly when blocked with excess NT (0.92 ± 0.20 %AD, $P < 0.01$, $t = 14.71$).

Micro-PET/CT Imaging

PC3-xenograft tumors were clearly visible as early as 0.5 h post-injection, and region of interest analysis showed tumor uptake of 4.53 ± 1.26 %ID/g (Fig. 3). The tumor-to-background ratio (5.61 ± 0.69) and tumor uptake (4.95 ± 0.67 %ID/g) at 1 h post-injection was significantly higher compared with blocking group (1.95 ± 0.17 %ID/g, $P < 0.01$, $t = 8.72$), demonstrating the specificity of ^{68}Ga-DOTA-NT-20.3 for NTR1-positive tumors. Quantitative analysis showed that radioactivity peaked in main organs such as heart, lung, brain, bone, and muscle early and then cleared over 1 h. Visualization of kidney and bladder showed no striking radioactivity in liver, confirming the tracer was rapidly excreted via urinary system. LNCap-tumor-bearing mice were used as a negative control, and PET imaging demonstrated minimal tumor accumulation of ^{68}Ga-DOTA-NT-20.3 (0.81 ± 0.06 %ID/g) (Fig. 4). ^{68}Ga-PSMA-11 was subsequently injected into PC3- and LNCap-xenograft mice, and high radioactivity uptake (8.60 ± 2.11 %ID/g) was detected in LNCap but not in PC3 tumors (0.53 ± 0.05 %ID/g). The results indicated that ^{68}Ga-DOTA-NT-20.3 specifically targeted NTR1 and could be a promising new tool to complement PSMA PET for the diagnosis of PCa.

Biodistribution

The metabolic characteristics and targeting specificity of ^{68}Ga-DOTA-NT-20.3 *in vivo* were further evaluated by biodistribution experiments in PC3 tumor models (Table 1). The highest tumor uptake (6.26 ± 0.41 %ID/g) was measured at 60 min post-injection and decreased slightly to 3.74 ± 0.56 %ID/g by 120 min. The radiotracer cleared quickly from blood and major organs (brain, heart, lung, liver, muscle, bone), with significantly high tumor-to-liver (4.41 ± 0.73) and tumor-to-muscle ratios (12.34 ± 1.32) at 60 min. As a consequence of renal excretion, kidney-uptake values at 30, 60 and 120 min post-injection

were 23.06 ± 1.94, 24.55 ± 0.98, and 26.08 ± 0.79 %ID/g, respectively, further supporting renal clearance as the primary metabolic pathway of ^{68}Ga-DOTA-NT-20.3.

Immunohistochemical, Immunofluorescent, and Histological Analyses

To further validate the NTR1 and PSMA expression in different types of PCa, immunohistochemistry was performed for tumor tissues. PC3 xenograft showed high NTR1 expression levels but no obvious PSMA expression (Fig. 5A and B), while LNCap tumors showed over-expression of PSMA rather than NTR1 (Fig. 5D and E). Tumor immunohistochemistry findings corresponded with the micro-PET/CT imaging results. H&E staining (Fig. 5C and F) revealed the different morphological features of PCa, with irregularly arranged tumor cells that varied in size, with deep staining, obvious atypia, and high mitotic rates. Strong red fluorescence was seen in PC3 cells, confirming the abundant NTR1 expression (Fig. 6).

DISCUSSION

Despite great progress in the clinical management of localized PCa, metastatic PCa treated with ADT inevitably develops resistance, leading to CRPC (*24*). Novel anti-androgens (enzalutamide or abiraterone) further prevent tumor progression by inhibiting the reactivated androgen/androgen receptor signaling in CRPC (*25,26*). However, prolonged inhibition of androgen/androgen receptor pathway converts 15-20 % CRPC into androgen-independent NEPC, with loss of canonical AR and PSMA expression, which clinically resulting in a rapidly progressive disease course and no significant increase of PSA, thus hindering its clinical diagnosis and therapy (*7*). PSMA PET/CT and radio-ligand therapy had limited values for more aggressive PSMA-negative PCa phenotypes in clinical practice. NT/NTR signaling, recruited as an alternative growth pathway in the absence of androgen receptor, plays a crucial role in the proliferation, migration and invasion of NEPC cells (*10*). Acute NTR1 expression is associated with neuroendocrine differentiation of PCa, making it a promising biomarker that may compensate for the PSMA-negativity of NEPC (*16*). Various radiopharmaceuticals developed to trace NTR1 *in vivo* may aid the early diagnosis, distant metastasis detection, endoradiotherapy, and mechanistic investigation of NEPC (*17*). For this purpose, we radiolabeled ^{68}Ga-DOTA-NT-20.3 as an NTR1-targeted radiotracer and evaluated its imaging ability in two PCa xenograft models (PC3 and LNCap).

^{68}Ga-DOTA-NT-20.3 was efficiently prepared using an iQS-TS automated module, with high yield and radiochemical purity. The tracer showed good stability *in vitro*, with a radiochemical purity ≥ 99% at 4 h after incubation in PBS or plasma, providing the basis for further biological evaluations. The lipophilicity of ^{68}Ga-DOTA-NT-20.3 was −3.68 ± 0.14, indicating favorable *in vivo* radiopharmacokinetics, demonstrated by its predominantly renal elimination with little radioactivity in the liver. We also verified the binding affinity and specificity of ^{68}Ga-DOTA-NT-20.3 to NTR1 in PC3 cells, which show high levels of NTR1 expression, and further verified the binding by immunofluorescence. ^{68}Ga-DOTA-NT-20.3 showed significant radioactivity accumulation in PC3 cells in a time-dependent manner. Its binding ability was effectively blocked by excess NT within a low-nanomolar range, verifying the specificity of ^{68}Ga-DOTA-NT-20.3 for NTR1 in PC3 cells *in vitro*. A high target (NTR1)-binding affinity is required for high tumor uptake and retention of the radiopeptide, as the basic premise of molecular imaging *in vivo*.

The specificity of ^{68}Ga-DOTA-NT-20.3 was further confirmed by PET imaging in both NTR1-positive/PSMA-negative PC3 and NTR1-negative/PSMA-positive LNCap tumor xenografts. The results showed high and specific accumulation of ^{68}Ga-DOTA-NT-20.3 in PC3 tumor lesions at all time points, but very low uptake in LNCap-derived tumors. The small molecular size of ^{68}Ga-DOTA-NT-20.3 and its hydrophilic nature enables fast clearance of radioactivity from the blood and non-target tissues, resulting in a high tumor-to-muscle ratio of 5.61 ± 0.69 at 1h after intravenous injection. Blocking successfully reduced the localization of ^{68}Ga-DOTA-NT-20.3 within the tumor due to the presence of excess of cold NT analogs, clearly demonstrating the receptor specificity of this imaging agent. However, the radioactivity uptake could not be completely blocked by NT with the blocking ratio of 60.03 ± 6.48 % (Fig. 3B). It may be due to insufficient amount of cold NT, and further verifications may be needed. In contrast, ^{68}Ga-PSMA-11 PET showed no uptake in PC3-derived tumors, but high uptake in LNCap-derived tumors. The different radioactivity uptakes in two different tumor models can be attributed to the different numbers of binding sites (NTR1 or PSMA) in PC3 and LNCap cells, respectively. Immunohistochemistry further confirmed high NTR1 expression in PC3-derived tumors and conversely high PSMA expression in LNCap-derived tumors.

^{68}Ga-DOTA-NT-20.3 showed a prolonged tumor-retention time up to 4 h and quicker clearance from the blood, heart, lung, liver, muscle, and other organs or tissues, except

kidney, which correlated well with the PET imaging findings. ^{68}Ga-DOTA-NT-20.3 predominantly cleared via the renal pathway, leading to accumulation in kidney and bladder. The radioactivity in bladder can be excreted through urine, which is conducive to the detection of para-vesical and prostatic bed lesions. Regretfully, kidney may become a dose-limited organ due to the slower clearance of ^{68}Ga-DOTA-NT-20.3. The exact mechanism is not clear, but efforts should be taken to reduce the renal retention and potential nephrotoxicity for future internal radioligand therapy. Biodistribution analysis indicated a high tumor-to-muscle ratio (12.34 ± 1.32) at 1 h post-injection, identifying ^{68}Ga-DOTA-NT-20.3 as a promising PET tracer for imaging NTR1-expressing tumors. However, compared with the high binding affinity *in vitro* (IC_{50} 7.59 ± 0.41 nmol/L), the radiotracer demonstrated moderate PC3 tumor uptake *in vivo* (6.26 ± 0.41 %ID/g at 1 h), suggesting that many other factors in addition to binding affinity may affect the tumor uptake. Further systematic investigations are therefore needed to improve the absolute tumor uptake.

CONCLUSION

This study showed that ^{68}Ga-DOTA-NT-20.3 has high affinity to NTR1 and favorable distribution and kinetics. The high contrast image of ^{68}Ga-DOTA-NT-20.3 in PC3-xenograft with NTR1-avid expression indicated its potential for detecting poorly differentiated or neuroendocrine differentiation of PCa. The high stability and long intra-tumor retention of ^{68}Ga-DOTA-NT-20.3 hold promise to be used for peptide-receptor radionuclide therapy of PCa by exchanging ^{68}Ga with the therapeutic radionuclide ^{177}Lu/^{225}Ac. In addition, ^{68}Ga-DOTA-NT-20.3 might be an alternative targeted radiopharmaceutical for identifying neuroendocrine differentiation of PCa. Further preclinical studies are warranted to explore the molecular mechanisms of NTR1 in this context.

DISCLOSURE

This work was supported by Jiangsu Provincial Key Research and Development Special Fund (BE2017612), Nanjing Medical and Health International Joint Research and Development Project (201911042), General Project of Science and Technology Development Fund of Nanjing Medical University (NMUB2019154), National Natural Science Foundation of China (82003532), and the second round of Nanjing Clinical Medical Center "Nanjing Nuclear Medicine Center". No other potential conflict of interest relevant to this article was reported.

ACKNOWLEDGMENT

We thank Susan Furness, PhD, from Liwen Bianji (Edanz) (www.liwenbianji.cn/) for editing the English text of a draft of this manuscript.

KEY POINTS

Question: Can ^{68}Ga-DOTA-NT-20.3 serve as a NTR1-targeted radiotracer for the detection of neuroendocrine differentiation in PSMA-negative prostate cancer?

Pertinent Findings: ^{68}Ga-DOTA-NT-20.3 can be an ideal PET tracer with favorable characteristics. ^{68}Ga-DOTA-NT-20.3 is stable *in vitro* and has high affinity to NTR1. Cellular uptake performed on PC3 prostate cancer cell line (NTR1-positive) demonstrated that the uptake is specific. High contrast images were achieved in PC3 tumor xenografts but not in NTR1-negative/PSMA-positive LNCap tumors.

Implications for Patient Care: ^{68}Ga-DOTA-NT-20.3 has merits in the detection of neuroendocrine differentiation in the prostate cancer, which may contribute to NTR1 based theranostics and provide the novel strategy for the management of neuroendocrine prostate cancer, especially for the neuroendocrine differentiation in mCRPC.

REFERENCES

1. Li X, Zeng XY. Advances in epidemiology of prostate cancer in China. *Cancer Research on Prevention and Treatment*. 2021;48:98-101.
2. Loeb S. Guideline of guidelines: prostate cancer screening. *BJU Int*. 2014;114:323-325.
3. Sardana G, Dowell B, Diamandis EP. Emerging biomarkers for the diagnosis and prognosis of prostate cancer. *Clin Chem*. 2008;54:1951-1960.
4. Thompson IM, Pauler DK, Goodman PJ, et al. Prevalence of prostate cancer among men with a prostate-specific antigen level < or =4.0 ng per milliliter. *N Engl J Med*. 2004;50:2239-2246.
5. Rowe SP, Johnson GB, Pomper MG, et al. Recent updates and developments in PET imaging of prostate cancer. *Abdom Radiol*. 2020;45:4063-4072.
6. Will L, Sonni I, Kopka K, Kratochwil C, Giesel FL, Haberkorn U. Radiolabeled prostate-specific membrane antigen small-molecule inhibitors. *Q J Nucl Med Mol Imaging*. 2017;61:168-180.
7. Yamada Y, Beltran H. Clinical and biological features of neuroendocrine prostate cancer. *Curr Oncol Rep*. 2021;23:15.
8. Hsu EC, Rice MA, Bermudez A, et al. Trop2 is a driver of metastatic prostate cancer with neuroendocrine phenotype via PARP1. *Proc Natl Acad Sci U S A*. 2020;117:2032-2042.
9. Wang HT, Yao YH, Li BG, Tang Y, Chang JW, Zhang J. Neuroendocrine prostate cancer (NEPC) progressing from conventional prostatic adenocarcinoma: factors associated with time to development of NEPC and survival from NEPC diagnosis-a systematic review and pooled analysis. *J Clin Oncol*. 2014;32:3383-3390.
10. Zhu S, Tian H, Niu X, et al. Neurotensin and its receptors mediate neuroendocrine transdifferentiation in prostate cancer. *Oncogene*. 2019;38:4875-4884.
11. Nikolaou S, Qiu S, Fiorentino F, et al. The role of neurotensin and its receptors in non-gastrointestinal cancers: a review. *Cell Commun Signal*. 2020;18:68.
12. Christou N, Blondy S, David V, et al. Neurotensin pathway in digestive cancers and clinical applications: an overview. *Cell Death Dis*. 2020;11:1027.
13. Tyler-McMahon BM, Boules M, Richelson E. Neurotensin: peptide for the next millennium. *Regul Pept*. 2000;93:125-136.
14. Huang JT, Wu CY, diSant'Agnese PA, Yao JL, Cheng L, Na YQ. Function and molecular mechanisms of neuroendocrine cells in prostate cancer. *Anal Quant Cytol Histol*. 2007;29:128-138.
15. Hashimoto K, Kyoda Y, Tanaka T, et al. The potential of neurotensin secreted from neuroendocrine tumor cells to promote gelsolin-mediated invasiveness of prostate adenocarcinoma cells. *Lab*

Invest. 2015;95:283-295.

16. He T, Wang M, Wang H, et al. Evaluation of neurotensin receptor 1 as potential biomarker for prostate cancer theranostic use. *Eur J Nucl Med Mol Imaging*. 2019;46:2199-2207.
17. Maschauer S, Prante O. Radiopharmaceuticals for imaging and endoradiotherapy of neurotensin receptor-positive tumors. *J Labelled Comp Radiopharm*. 2018;61:309-325.
18. Teodoro R, Faintuch BL, Fernández Núñez EG, Guimarães Queiróz R. Neurotensin (8-13) analogue: radiolabeling and biological evaluation using different chelators. *Nucl Med Biol*. 2011;38:113-120.
19. Wu Z, Li L, Liu S, et al. Facile preparation of a thiol-reactive 18F-labeling agent and synthesis of 18F-DEG-VS-NT for PET imaging of a neurotensin receptor-positive tumor. *J Nucl Med*. 2014;55:1178-1184.
20. Deng HF, Wang H, Wang MZ, Li ZB, Wu ZH. Synthesis and evaluation of 64Cu-DOTA-NT-Cy5.5 as a dual-modality PET/fluorescence probe to image neurotensin receptor-positive tumor. *Mol Pharm*. 2015;12:3054-3061.
21. Alshoukr F, Prignon A, Brans L, et al. Novel DOTA-neurotensin analogues for 111In scintigraphy and 68Ga PET imaging of neurotensin receptor-positive tumors. *Bioconjug Chem*. 2011;22:1374-1385.
22. Prignon A, Provost C, Alshoukr F, et al. Preclinical evaluation of 68Ga-DOTA-NT-20.3: A promising PET imaging probe to discriminate human pancreatic ductal adenocarcinoma from pancreatitis. *Mol Pharm*. 2019;16:2776-2784.
23. Zhang LL, Li WC, Xu Z, et al. ^{68}Ga-PSMA PET/CT targeted biopsy for the diagnosis of clinically significant prostate cancer compared with transrectal ultrasound guided biopsy: a prospective randomized single-centre study. *Eur J Nucl Med Mol Imaging*. 2021;48:483-492.
24. Friedlander TW, Ryan CJ. Targeting the androgen receptor. *Urol Clin North Am*. 2012;39:453-464.
25. de Bono JS, Logothetis CJ, Molina A, et al. Abiraterone and increased survival in metastatic prostate cancer. *N Engl J Med*. 2011;364:1995-2005.
26. Beer TM, Armstrong AJ, Rathkopf DE, et al. Enzalutamide in metastatic prostate cancer before chemotherapy. *N Engl J Med*. 2014;371:424-433.

Table 1. Biodistribution of ^{68}Ga-DOTA-NT-20.3 in PC3 tumor-bearing mice at various time points post injection (%ID/g, mean ± SD, n = 3).

Part	5min	15min	30min	60min	120min
Blood	8.11 ± 1.54	4.15 ± 0.59	2.56 ± 0.23	1.12 ± 0.22	0.43 ± 0.08
Heart	7.70 ± 0.90	3.88 ± 0.18	2.78 ± 0.36	1.57 ± 0.18	0.58 ± 0.11
Liver	5.46 ± 1.01	3.17 ± 0.45	2.02 ± 0.48	1.44 ± 0.20	0.86 ± 0.49
Spleen	3.97 ± 0.39	2.81 ± 0.47	1.85 ± 0.43	1.06 ± 0.27	0.41 ± 0.04
Lung	5.18 ± 0.16	3.28 ± 0.62	1.91 ± 0.15	1.20 ± 0.23	0.75 ± 0.15
Kidney	18.36 ± 1.27	21.22 ± 1.95	23.06 ± 1.94	24.55 ± 0.98	26.08 ± 0.79
Stomach	3.56 ± 0.31	2.49 ± 0.35	1.75 ± 0.38	0.91 ± 0.18	0.37 ± 0.05
Intestine	3.28 ± 0.30	2.31 ± 0.92	1.47 ± 0.26	0.77 ± 0.24	0.38 ± 0.04
Pancreas	2.88 ± 0.61	2.03 ± 0.26	1.59 ± 0.60	1.05 ± 0.07	0.36 ± 0.04
Muscle	1.93 ± 0.65	1.44 ± 0.17	0.96 ± 0.08	0.51 ± 0.02	0.32 ± 0.04
Bone	2.27 ± 0.29	2.35 ± 0.52	1.27 ± 0.08	0.86 ± 0.17	0.53 ± 0.17
Brain	1.91 ± 0.39	1.35 ± 0.15	0.88 ± 0.10	0.60 ± 0.05	0.33 ± 0.10
Fat	1.42 ± 0.23	1.11 ± 0.23	0.62 ± 0.11	0.32 ± 0.03	0.32 ± 0.07
Testis	1.62 ± 0.11	1.31 ± 0.05	0.80 ± 0.06	0.42 ± 0.04	0.31 ± 0.10
Tumor	2.81 ± 0.39	3.93 ± 0.43	5.70 ± 0.80	6.26 ± 0.41	3.74 ± 0.56

Figure Legends

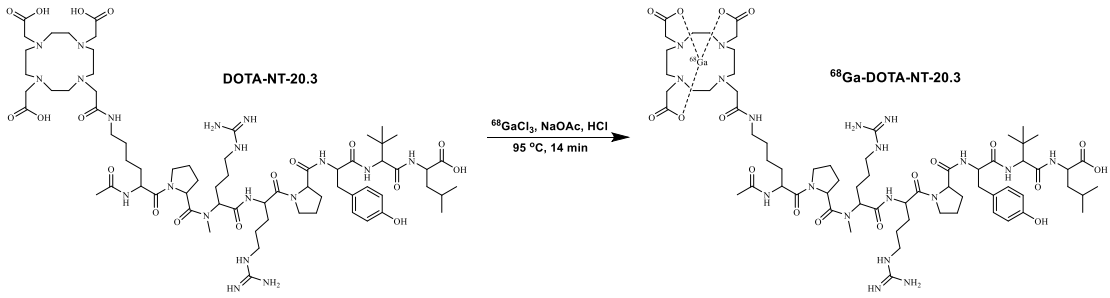

Figure 1. Radiosynthesis and structure of ^{68}Ga-DOTA-NT-20.3.

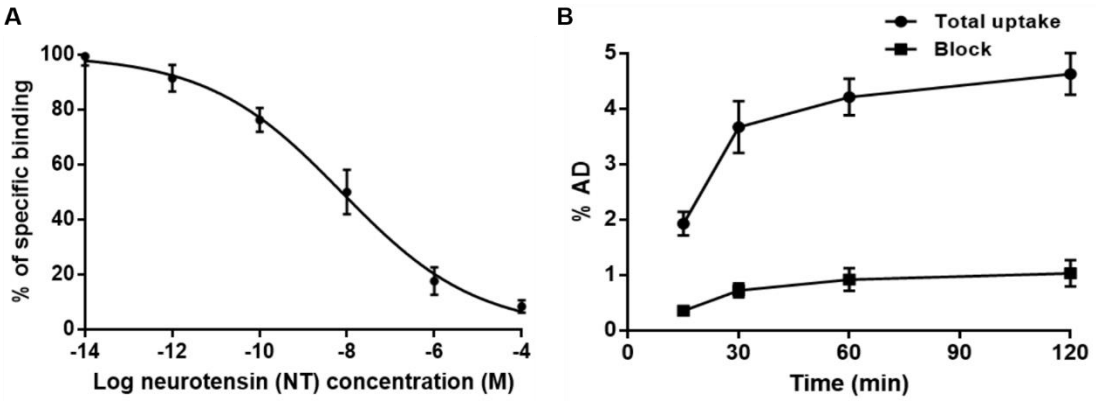

437

438 **Figure 2. (A) Competitive binding curves for IC_{50} determination of ^{68}Ga-DOTA-NT-20.3 in PC3**
439 **cells, using NT as a competitive inhibitor. (B) Uptake of ^{68}Ga-DOTA-NT-20.3 in PC3 cells.**
440

441

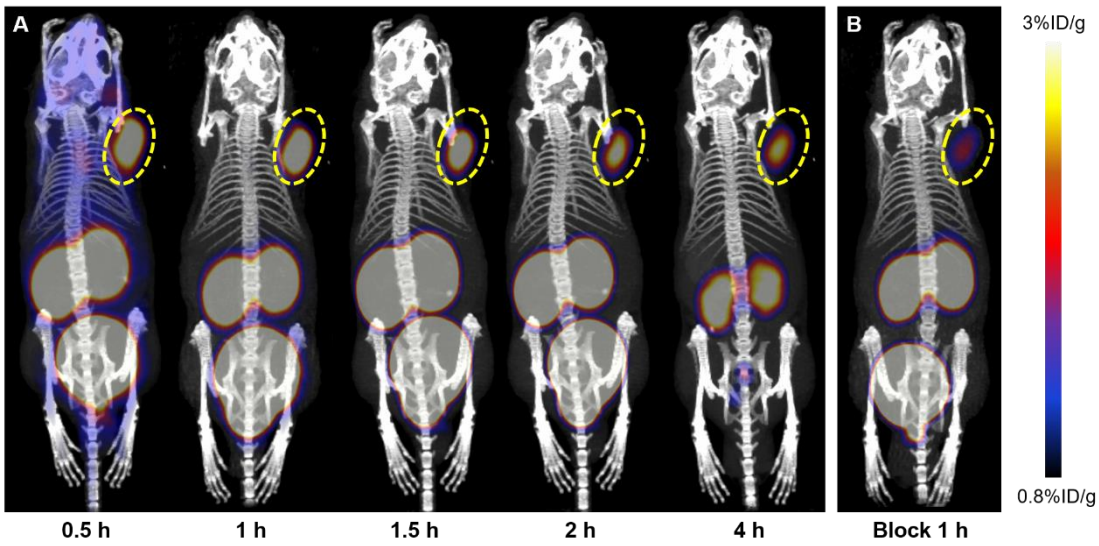

Figure 3. (A) Micro-PET/CT images of PC3 tumor-bearing mice at different time points after injection of ^{68}Ga-DOTA-NT-20.3. (B) Blocked by excess NT at 1 h post injection of ^{68}Ga-DOTA-NT-20.3, the blocking ratio [(total radioactivity uptake - blocked radioactivity uptake) / total radioactivity uptake] was 60.03 ± 6.48 %.

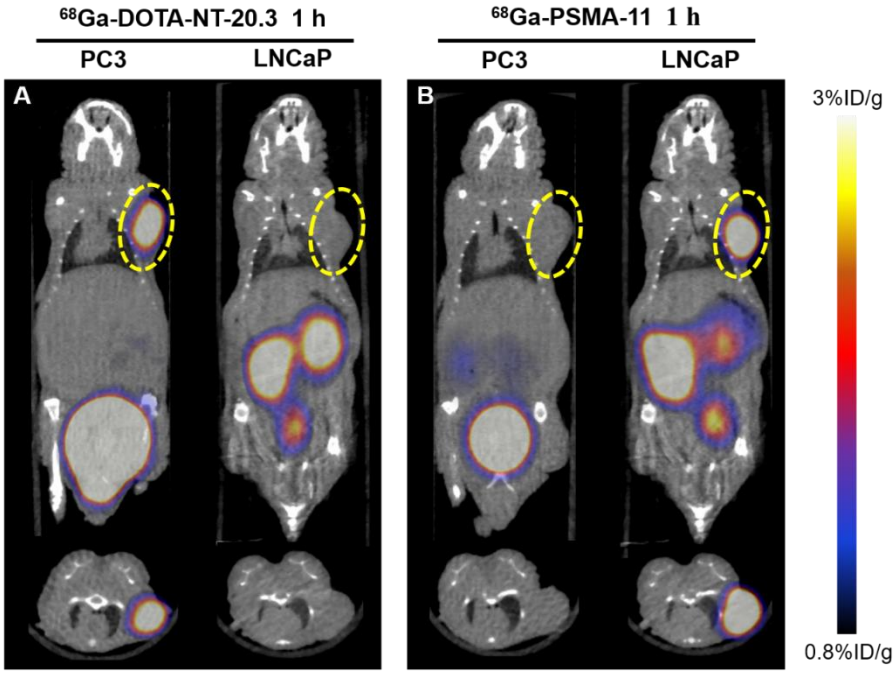

Figure 4. Micro-PET/CT images of PC3 and LNCap tumor-bearing mice at 1 h post injection of ^{68}Ga-DOTA-NT-20.3 (A) or ^{68}Ga-PSMA-11 (B).

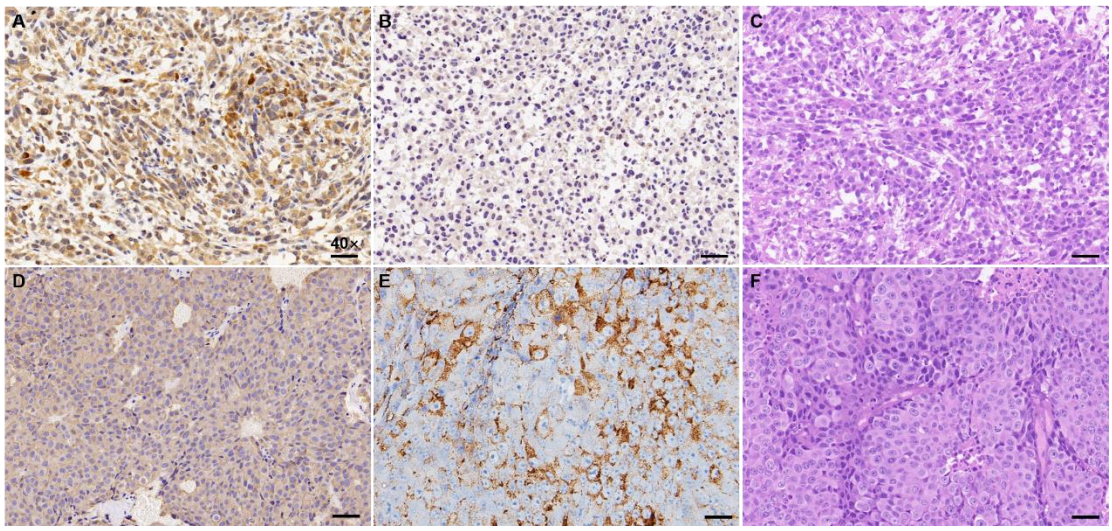

Figure 5. Representative immunohistochemical and histological images. (A-C) NTR1 and PSMA immunohistochemical, and H&E staining of PC3 tumors. (D-F) NTR1 and PSMA immunohistochemical, and H&E staining of LNCap tumors. (scale bar, 10 µm; ×40).

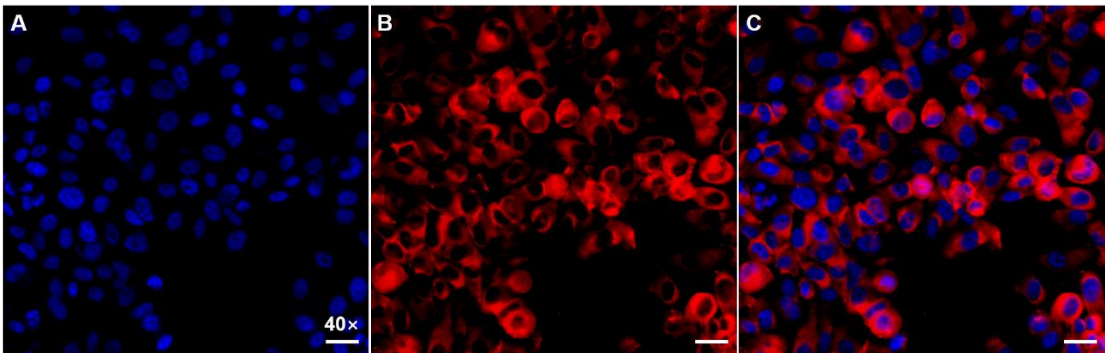

Figure 6. Representative immunofluorescence images. PC3 cells were incubated with fluorescent NTR1 antibody (red) and nuclei were stained with DAPI (blue). DAPI, 4-6-diamidino-2-phenylindole. (scale bar, 10 μm; ×40).

GRAPHICAL ABSTRACT

NTR1 Expression Imaging with ^{68}Ga-DOTA-NT-20.3

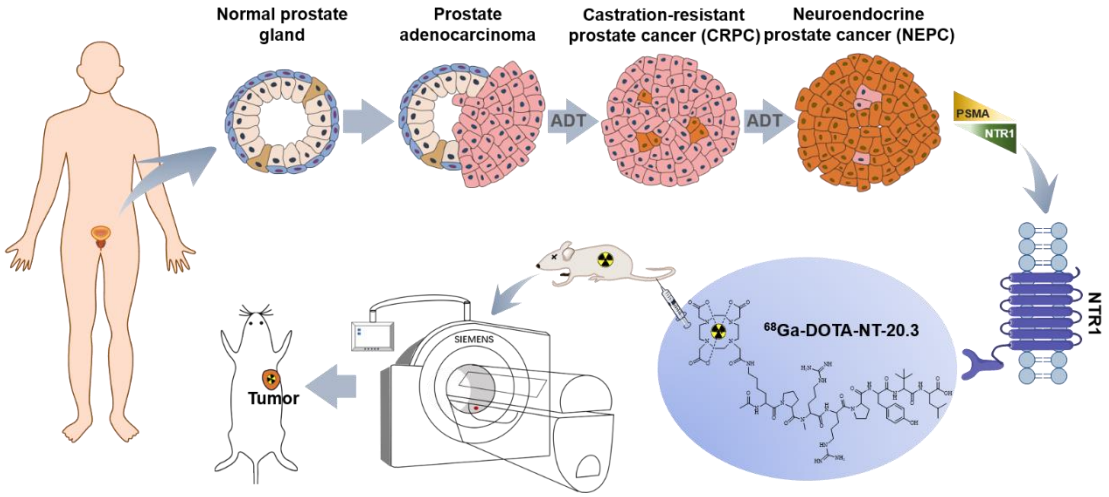

SUPPLEMENTAL DATA

Glossary

Acronym	Full name
ADT	Androgen-deprivation therapy
BSA	Bovine serum albumin
DOTA	1,4,7,10-tetraazacyclododecane-1,4,7,10-tetraacetic acid
Micro-PET/CT	Micro-positron emission tomography/computed tomography
PBS	Phosphate-buffered saline
PSA	Prostate specific antigen
PSMA	Prostate-specific membrane antigen
Radio-HPLC	Radio-high-performance liquid chromatography
Radio-TLC	Radio-thin layer chromatography

Materials

All commercially obtained chemicals were of analytical grade and were used without further purification. DOTA-NT-20.3 peptide [Ac-Lys(1,4,7,10-tetraazacyclododecane-1,4,7,10-tetraacetic acid)-Pro-(NMe-Arg)-Arg-Pro-Tyr-Tle-Leu] was kindly provided by Iason GmbH (Graz, Austria). PSMA-11 and NT were purchased from ABX (Radeberg, Germany) and Aladdin (Shanghai, China), respectively. Sodium acetate and hydrochloric acid were obtained from Merck (Darmstadt, Germany). 0.9% sodium chloride injection was provided by Otsuka (China). An ITG Ge-68/Ga-68 Generator and iQS-theranostics synthesizer (iQS-TS) automated module (ITG GmbH, Munich, Germany) were used. The peptide was analyzed using a Shimadzu HPLC system with a C18 column (5μm, 250 mm × 10 mm; Waters Xbridge C18, Milford, MA, USA). ^{68}Ga-radioactivity (400-600 keV) was measured with a gamma counter (Wizard 2; PerkinElmer, USA). Imaging *in vivo* was carried out with Inveon micro-PET/CT (Siemens Medical Solutions, Germany) and reconstructed with Inveon Research Work Station.

Tumor Cell Lines and Mouse Models

Human prostate adenocarcinoma PC3 and LNCap cells were obtained from the Cell Bank of Shanghai Institutes for Biological Sciences and cultured in medium containing 10 % fetal bovine serum (Gibco, Grand Island, NY, USA) and 1% penicillin–streptomycin solution 100 U/mL (Beyotime, Shanghai, China). All cell lines were incubated at 37 °C in a humidified incubator with 5 % CO_2 and used for subsequent experiments during

logarithmic growth. Animal experiments were performed using (4−6)-week-old male BALB/c nude mice (18-25g, BioHermes, Wuxi, China). To establish PCa models, mice were injected in their right armpits with a single-cell suspension of 2×10^6 PC3 or LNCap cells. When the tumor volume reached 200mm^3, the mice were subjected to PET imaging and biodistribution analysis. Isoflurane (RWD, Shenzhen, China) served as anesthetic for animal use.

Quality Control

The radiolabeling yield and radiochemical purity of ^{68}Ga-DOTA-NT-20.3 and ^{68}Ga-PSMA-11 were detected with a flow-count radio-HPLC detector (B-FC-1000F, Bioscan, DC, USA). Elution was performed with a mixture of A (0.1% trifluoroacetic acid (TFA) in water) and B (0.1% TFA in acetonitrile) with a flow rate of 1 mL/min. The linear gradient elution of ^{68}Ga-DOTA-NT-20.3 started from 100%–90% A for 5 min, and then changed linearly to 90%–20% A for 15 min. Finally, the mobile phase returned linearly to 100% B at the run end, and the retention time of ^{68}Ga-DOTA-NT-20.3 was 13.61 ± 0.12 min. ^{68}Ga-PSMA-11 elution was carried out with a linear gradient of A from 80 % to 20% within 15 min, and the retention time was 8.16 ± 0.13 min. Radiochemical purity of ^{68}Ga-DOTA-NT-20.3 was also accessed by a B-AR-2000 radio-TLC imaging scanner (Bioscan) using the silica gel impregnated iTLC-SG-Glass microfiber chromatography papers (Agilent, CA, USA). The developing solvent was methanol and 1 M sodium acetate (1 : 1), and the retention factor of ^{68}Ga-DOTA-NT-20.3 was 0.60 ± 0.02.

Supplemental Figure

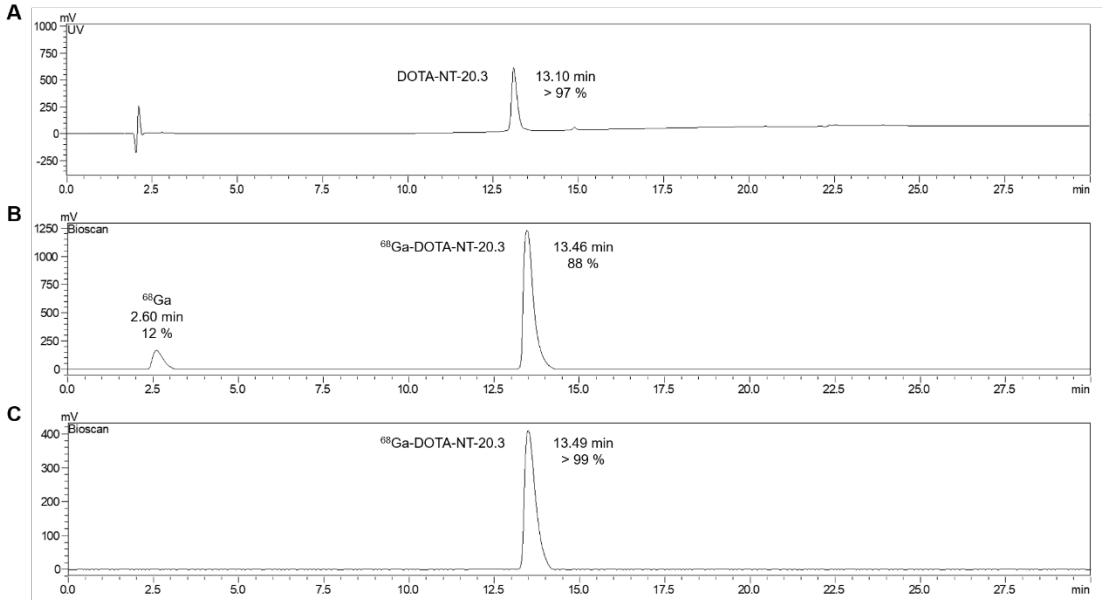

Supplemental Figure 1. (A) HPLC analysis of DOTA-NT-20.3. (B, C) Radiolabeling yield and radiochemical purity of ^{68}Ga-DOTA-NT-20.3 analyzed by radio-HPLC.

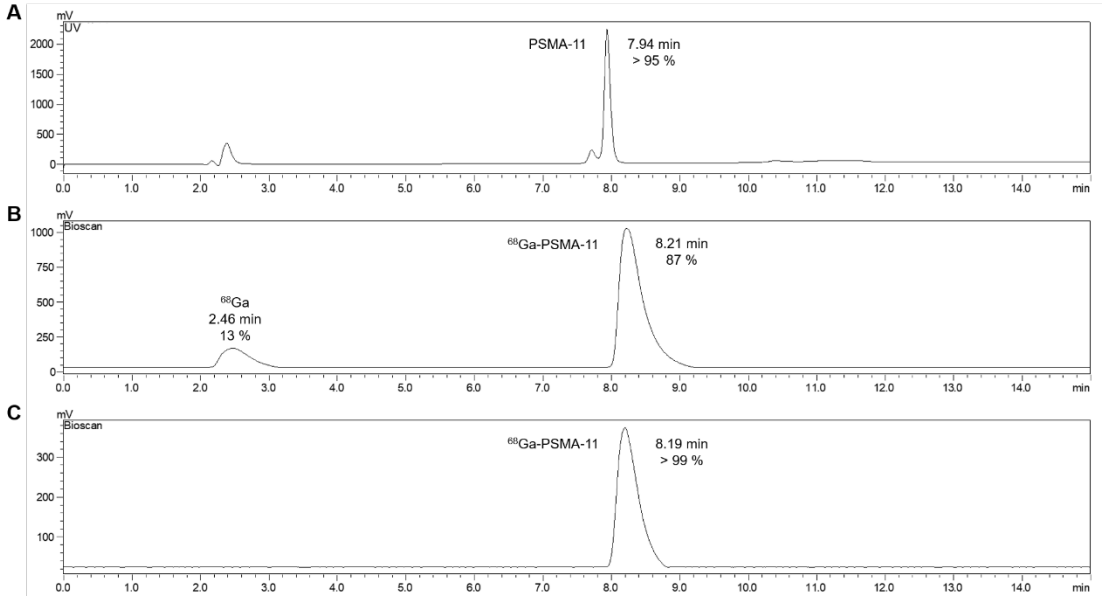

Supplemental Figure 2. (A) HPLC analysis of PSMA-11. (B, C) Radiolabeling yield and radiochemical purity of ^{68}Ga- PSMA-11 analyzed by radio-HPLC.

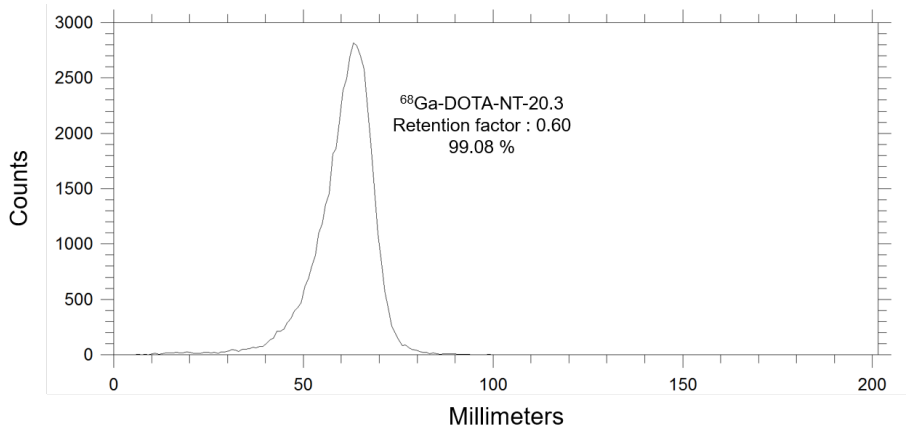

Supplemental Figure 3. Radiochemical purity of ^{68}Ga-DOTA-NT-20.3 analyzed by radio-TLC.

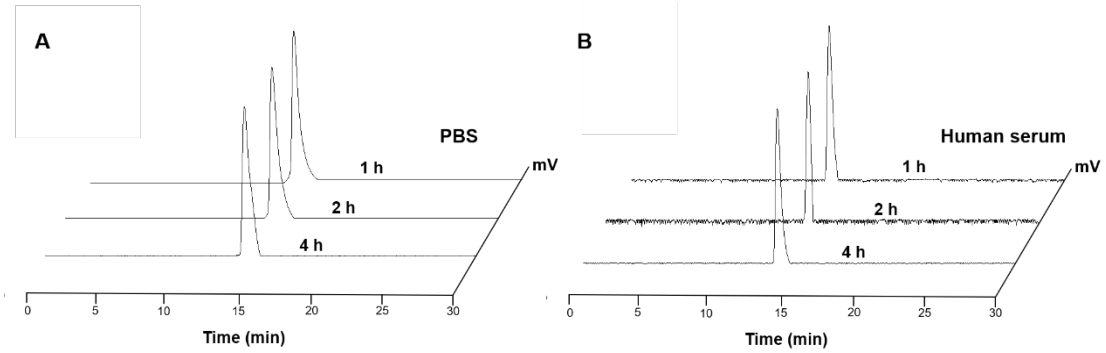

Supplemental Figure 4. In vitro stability of ^{68}Ga-DOTA-NT-20.3 in PBS (A) and human serum (B), respectively, 1, 2, and 4 h after incubation.